Signaling the agency of an erroneous outcome via synchronization of spikes in the cerebellum

Jay S. Pi, Ehsan Sedaghat-Nejad, Mohammad Amin Fakharian,
Paul Hage, and Reza Shadmehr

Laboratory for Computational Motor Control, Dept. of Biomedical Engineering
Johns Hopkins School of Medicine, Baltimore, Maryland USA

Correspondence: Reza Shadmehr or Jay S. Pi, Johns Hopkins School of Medicine, 410 Traylor Building, 720 Rutland Ave., Baltimore, MD 21205.
Email: shadmehr@jhu.edu or jay.s.314159@gmail.com

Acknowledgements: The work was supported by grants from the National Science Foundation (CNS-1714623), the NIH (R01-EB028156, R01-NS078311), and the Office of Naval Research (N00014-15-1-2312).

Author contributions: J.S.P., E.S.H, P.H., and R.S. conceived and performed experiments. J.S.P., E.S.N., M.A.F., and R.S. analyzed data, J.S.P. made figures and performed statistical analysis. R.S. wrote the manuscript.

Competing interests: None.

Abstract

Claiming agency is a prerequisite for taking responsibility: the brain must differentiate between the sensory events that are the erroneous consequences of our actions, and thus may be remedied if we change our behavior, and the many other events in our environment that consume our attention, but for which we have no means of influence. In the cerebellum, the firing rates of complex spikes of Purkinje cells signal that a sensory or a motor event has taken place, but do not specify if that event was the consequence of the animal's action. Instead, to claim agency of a sensory outcome, the complex spikes synchronize within the population of Purkinje cells that guided that action. As a result, in the cerebellum the erroneous sensory consequences of movements are identified not via modulation of complex spike firing rates, but via synchronization of spikes.

Introduction

We attend to numerous sensory events around us, recognizing that only a fraction are the consequences of our own actions. Identifying which sensory events are our responsibility, and which are beyond our means of influence, is a first step in generating a learning signal that can improve our behavior. How does the brain differentiate between the sensory events for which we have agency, and thus can change by altering our behavior, and those that we attend to, but for which we have no means of influence?

The cerebellum provides an important substrate to investigate this question because motor learning implicitly requires a sense of agency: we must believe that a sensory event was the consequence of our movement before we invest the resources that promote learning from the sensory prediction errors. Indeed, theories of cerebellar function suggest that we learn how to move because the inferior olive provides a teaching signal to the Purkinje cells (P-cells) of the cerebellum (*1*, *2*), controlling the rates of complex spikes (CS) to indicate that the sensory consequences of a movement were in error (*3*–*5*). However, these rate changes are not specific to erroneous movements (*6*). Rather, the CS rates change in response to a variety of sensory events (*7*–*12*), and before a variety of movements (*13*–*17*).

For example, CS rates are modulated by the touch of a limb (*18*), an air puff to the face (*9*, *10*, *19*), or sudden presentation of a visual stimulus (*8*, *20*), signaling that a salient sensory event has occurred (*9*, *12*), particularly one that is rewarding (*11*). Moreover, CS rates are modulated before the onset of motor events such as walking (*15*), licking (*13*), reaching (*14*, *16*, *17*), and moving the wrist (*21*). Indeed, production of CSs, either through the action of the drug harmaline (*22*), or the stimulation of climbing fibers (*23*), generates movements. This rich diversity of events that modulate CS rates raises a critical problem for theories that view the cerebellum as a learning machine (*24*, *25*): how does the cerebellum distinguish the erroneous consequences of a movement in a signal that generously responds to both sensory and motor events?

During simultaneous recordings from many P-cells in a non-human primate (marmosets), we observed that the erroneous sensory consequences of saccades were sent to the cerebellum not via modulation of CS firing rates, but via synchronization of CS timing in the population of P-cells that was responsible for guiding that saccade. Before a movement began, both the sensory event that instructed the movement, and the movement itself, were accompanied with CS rate modulation. However, if the movement resulted in an erroneous outcome, then that sensory event caused the olive to re-engage the P-cells, again producing CS rate modulation, but now synchronously.

Results

Inspired by the behavioral work of Wallman and Fuchs (*26*) and Tseng et al. (*27*), we designed a 2x2 task in which a visual event was sometimes but not always followed by a movement, and a movement that was sometimes but not always preceded by a visual event (Fig. 1C). Some of the visual events were unpredictable, producing sensory prediction errors (SPEs), while others were predictable. Critically, only one of the SPEs signaled the erroneous outcome of a movement.

Marmosets fixated at a center location and were presented with a primary target at a random direction (Fig. 1A). As the primary saccade commenced, we moved the target to a secondary location, also at a random direction (Fig. 1B). To assign a value to this erroneous outcome, in 51% of the sessions reward required both the primary and the corrective saccades, whereas in the remaining sessions reward required only the primary saccade. If reward did not require the corrective saccade, the secondary target was presented only briefly and returned to the primary location (~120 ms, adjusted during the recording session). Following 200 ms fixation of the final target, the center target was presented, and the subject made a back-to-center saccade. Thus, the primary target was an unpredictable sensory event that instructed a movement. The center target also instructed a movement, but was predictable. The secondary target was unpredictable, but only sometimes instructed a movement. However, the secondary target was the sole event that indicated the erroneous consequences of a movement.

We used MRI and CT guided targeting procedures (*28*) to place tetrodes, heptodes, and silicon probes in lobules VI and VII of the vermis and recorded from n=268 saccade modulated P-cells. In every case, the neuron was identified as a P-cell because of the presence of CSs. For each type of visual event (primary, secondary, and center target), we estimated the direction that produced the largest increase in CS firing rates and labeled it as CS-on (Fig. S1A). The CS-on direction remained consistent across the various visual events (Fig. S1C). Thus, we combined the CS response for all visual events and defined the CS-on direction of each P-cell. The CS-on direction varied approximately with the cell's location in the vermis (Fig. S1B) (*8*, *29*).

Presentation of the primary target in direction CS-on produced a sharp increase in CS rates at 65.9±0.28 ms, and then a broad increase at 130 ms (Fig. 1D). In contrast, when the primary target was in direction CS+180, the CS rates were suppressed below baseline at around 87.1±3.3 ms latency. This direction-dependent response was also present when the data were aligned to saccade onset. When the saccade was delayed because of a long reaction time, the CS rate modulation remained, but became weaker in response to the visual stimulus, and before the saccade (Fig. S2A). Occasionally, the primary target was presented but the subject made a saccade in a different direction (Fig. S2B). In this case, the olive continued to response to the visual event at 70 ms latency (Fig. S2B), but the later response at 130 ms vanished. However, before task irrelevant saccades (Fig. 1D) the CS rate modulation was considerably weaker (50ms period before saccade onset, Wilcoxon signed rank, $z=6.15$, $p<10^{-6}$). Thus, the CS rates were modulated both in response to the visual events, and by the movements that followed those visual events.

Both the primary and the secondary targets were unpredictable. However, only the secondary target indicated the erroneous consequences of a movement, i.e., an event that induces motor learning (*5*). We considered all trials (in all sessions) in which the subject made a corrective saccade and found that paradoxically, the CS-on rates were actually weaker following the secondary target as compared to

the primary target (25-75ms post target onset, Wilcoxon signed rank, $z=5.79$, $p<10^{-6}$). Unlike the primary and secondary targets, both the onset and the position of the center target were predictable. As a result, the reaction times were shorter for the center saccades (median of 159 vs. 170 ms, Wilcoxon rank sum, $z=50.26$, $p<10^{-8}$). Yet, the CS response to the center target was similar to the primary target (Fig. 1D). Thus, the CS rates were modulated following both predictable and unpredictable visual events. Notably, the CS rates could not identify the visual event that indicated the erroneous consequences of a movement.

Our data included n=99 pairs of simultaneously isolated P-cells in which we computed the probability of synchronously timed CSs, corrected for chance (*29*). Because the CS rates were extremely low (Fig. S1A), we collapsed the trials across directions and found that at baseline, CS synchrony was roughly two times greater than chance (*30*). However, unlike the firing rates, the probability of synchrony did not change in response to the primary or center targets, nor did it change before the onset of the primary or center saccades (Fig. 1E). Remarkably, CS synchrony increased following the secondary target: it reached a peak at around 80 ms after the secondary target (50-100ms after visual event, secondary vs. primary target, Wilcoxon signed rank, $z=4.27$, $p=0.00038$), and 40 ms before the onset of the corrective saccade (25-75ms before onset, Wilcoxon signed rank, $z=2.95$, $p=0.017$). Thus, whereas CS rates were strongly modulated following the onset of the primary and center targets, and before the onset of the primary and center saccades, none of these sensory or motor events affected CS synchrony. Instead, CS synchrony increased only following the sensory event that signaled the erroneous consequences of a movement.

We were concerned that CS synchronization may be unrelated to the secondary target, and merely an event associated with the conclusion of a saccade. To check for this, we aligned the data to the termination of the various saccades and found that synchronization increased only after the primary saccade, i.e., when the erroneous sensory event was experienced, but not after other saccades (Fig. S3). In addition, because the secondary saccades were smaller in amplitude than other saccades, synchronization may have been an artifact of this difference. Thus, we selected a subset of the center saccades that had similar amplitudes as the corrective saccades and found that CS synchronization remained greater for the corrective saccades (Fig. S4, 100ms period following visual onset, Wilcoxon signed rank, $z=5.72$, $p=2\times10^{-6}$).

We next devalued the erroneous sensory consequences of the movement: in some sessions the secondary target was presented briefly (119±59 ms, mean±SD) and reward acquisition no longer required making a corrective saccade. As a result, in only 35±15% of trials the subjects made the correction, while in the remaining trials they ignored the secondary target. This devaluation of the sensory event altered the CS rates: when the secondary target was in direction CS-on, even in trials in which the corrective saccade was made the CS rates no longer exhibited the sharp increase at 70 ms (Figs. 2A & 2C, comparison of sessions in which the corrective saccade was required to optional, 100 ms following target onset, Wilcoxon rank sum, $z=3.08$, $p=0.0047$). Indeed, the rates exhibited a brief suppression in trials in which the subjects chose to ignore the secondary target (Fig. 2A, first row). Thus, devaluing the secondary target suppressed the CS rates (*11*, *16*, *31*), and the rates were further suppressed if the decision was to withhold the corrective saccade. While this devaluation of the sensory event led to reduced CS rates, if the subject chose to respond to it, then the CSs synchronized in response to the target (Fig. 2B, 50-100 ms period, comparison with primary target, Wilcoxon signed

rank, z=5.01, p=0.000026), and before the onset of the corrective saccade (25-100 ms period, comparison with primary saccade, Wilcoxon signed rank, z=3.89, p=0.00256). Remarkably, even if the subject chose to ignore the secondary target, the CSs were still more synchronized than in response to the primary target (50-100 ms period, Wilcoxon signed rank test, z=4.82, $p=1.2x10^{-5}$).

But how might CSs synchronize in response to only the secondary target? In our experiment, the secondary target was a visual event that followed a saccade, whereas all the other visual events took place during fixation. The origin of CS synchrony is the gap junctions of the inferior olive (*32*), which are more synchronized during movements vs. rest (*33*). Thus, the production of a movement may alter the state of the olive, making it more prone to synchronization. One way that this can occur is that the simple spikes (SS) that are produced during a movement (*29*) may influence not only the ongoing saccade via the fastigial nucleus neurons that project to the brainstem burst generators (*34*), but also change the state of the inferior olive through nucleo-olive projections (*35*, *36*). To check for this, we asked whether the SS activity of the P-cells had any influence on the subsequent probability of CS synchrony.

The primary and center targets were presented when the subject was fixating. During fixation, the SS rates were suppressed below baseline, even when no CSs were present (Fig. 3A). The presentation of a visual target strongly modulated the CS rates (Fig. 1D) but had no effects on the SS rates (Fig. 3C). Instead, at around 80 ms following the visual stimulus the SS rates returned to baseline, presumably reflecting the end of the fixation period and the prelude to a saccade. In contrast to the apparent lack of an SS response to the visual events, the SS rates were strongly modulated by movements. Before saccade onset, the rates rose above baseline and produced a burst (Fig. 3C). In direction CS+180, the burst was followed by a brief pause that was timed with deceleration onset. Thus, in contrast to the CS rates that were modulated by both visual and motor events, the SS rates were modulated by movements but not visual events.

At baseline, the SS synchronization index was between 1.25 and 1.50 (Fig. 3D), demonstrating that SS timing in neighboring P-cells was 25-50% more synchronized than would be expected by chance. SS synchronization did not change following the onset of the primary target (Fig. 3C). Rather, SS synchronization increased during movements, particularly at deceleration onset in direction CS+180 (*29*). Despite the fact that P-cells are inhibitory neurons, a synchronous SS in a population of P-cells can entrain the nucleus neurons, making them fire (*37*), re-setting the phase of the membrane oscillations in the inferior olive cells that produce the CSs (*38*). Thus, we asked whether the synchronous CS response to the secondary target was influenced by the probability of SS synchrony in the preceding primary saccade.

We divided the primary saccades based on whether they exhibited a synchronous SS event in the 100 ms period before saccade end and found that if the primary saccade included a synchronous SS event, then the CS response to the secondary target was more synchronous (Fig. 4A, left subplot, 200ms period from visual onset, Wilcoxon signed rank z=5.32 $p=1x10^{-6}$). However, because SS synchrony varied with the direction of the primary saccade, this result may have been simply an effect of saccade direction. Thus, we focused on the primary saccades that were in direction CS+180, the direction that exhibited the greatest probability of SS synchrony, and again divided the primary saccades based on the presence or absence of a synchronous SS event. Remarkably, primary saccades that had included a synchronous SS event were followed by a multi-peaked, synchronous CS response to the secondary

target (Fig. 4A, right subplot, 200ms period from visual onset, Wilcoxon signed rank z=2.93 p=0.027). Moreover, these primary saccades also exhibited a sharp peak in CS synchrony near saccade end (arrow, Fig. 4A), at around the time that SS synchrony tends to be greatest. As a result, the CSs exhibited greater synchrony in response to the erroneous sensory consequences of the primary saccade when the primary saccade itself included a synchronous SS event.

Discussion

The input from the inferior olive to the cerebellum conveys information that guides learning (*39*, *40*), but this same input also provides information about diverse sensory and motor events that are not errors (*7*, *10*, *12*). In our task, we observed that the olivary input to P-cells was modulated following the onset of visual targets, and before the onset of saccades towards those targets (*20*, *41*). Notably, the CS firing rates were modulated regardless of whether the visual event indicated a movement error or not. These rate modulations were quite sensitive to the reward value of the stimulus: CS firing rates were suppressed when the stimulus was devalued, particularly if the animal withheld a movement toward it. Yet, the CS rates could not distinguish the erroneous consequences of a movement from other events.

To signal that the visual event was the erroneous consequences of a movement, the CSs became synchronized. The probability of CS synchrony was greater if the visual event followed a movement that itself had a synchronous SS event. Given that the P-cells exhibited SS modulation only during movements, and not in response to the visual events (Fig. 3C), the results suggest that the input that the inferior olive receives during the primary saccade from the cerebellum sets the stage so that if that movement is followed by a visual event, then the olivary cells will respond synchronously (Fig. 4B). As a result, agency is established via a sequence of events: SS synchrony during a movement, followed by CS synchrony in response to the sensory feedback that the olive receives after that movement. In this way, CS synchrony appears to dissociate erroneous sensory consequences from other sensorimotor events.

Why does the olive respond synchronously to the erroneous consequences of the movement?

The origin of CS synchrony is the gap junctions of the inferior olive (*32*), which are more synchronized during movements (vs. rest), and become even more synchronized if a perturbation disrupts the movement (*33*). In our experiment, all visual events took place during fixation, except for the secondary target, which followed a saccade. During fixation the SS rates were suppressed below baseline, and the SS synchrony was at baseline. In contrast, during saccades the SS rates were not only modulated, they were also more synchronized, especially when the saccade was in direction CS+180. SS synchrony tends to entrain nucleus neurons (*37*), making them fire. It is possible that the SS synchronization that occurs during a saccade not only steers the ongoing movement via the output from the fastigial nucleus to the saccade burst generators (*34*), but also alters the state of the inferior olive through nucleo-olive projections (*35*), resetting the phase of their subthreshold membrane potentials (*38*, *42*).

When the primary saccade ends and the secondary target is presented, that sensory event again engages the neurons in the superior colliculus, which in turn transmit their information to the inferior olive, producing modulation of the CS rates. However, the SS synchrony in the primary saccade, if indeed is transmitted to the olive, may make the olivary neurons respond more synchronously to the secondary target. Consistent with this view, we found that if the primary saccade included a

synchronous SS event, then in the same P-cells, the CS response to the secondary target tended to be more synchronous.

A role for the cerebellum during holding still

We found that the SS rates were suppressed below baseline during task-relevant fixations, but not when fixations were spontaneous and task-irrelevant. This suggests that the oculomotor regions of the vermis play an active role both during control of saccades, and during control of fixation (*43*). Our observations shed light on a recently reported clinical symptom termed "fixation nystagmus" in which patients exhibit nystagmus while fixating a visual target, but not during other periods of fixation (*44*). Indeed, a major symptom of cerebellar damage is loss of muscle tone, which is manifested during the active process of holding still (*45*). Our results predict that in arm regions of the cerebellum, the P-cell SS rates may also be suppressed when the subject is actively holding the arm still (e.g., against gravity).

A role for the cerebellum during movements

It has been noted that the SS rates correlate with kinematic variables like position and/or velocity (*46*–*49*), but because such signals often correlate with the motor commands, it is not clear whether the P-cell output is a prediction of the sensory consequences, or the motor commands needed to generate a desired sensory consequence (*50*). Previously we reported that the SS rates exhibited a burst before saccade onset, but then fell below baseline and synchronized around the onset of deceleration (*29*). The magnitude of the burst grew with saccade velocity, but the timing of the pause remained locked to deceleration onset, especially when the saccade was in direction CS+180. The CS-on direction of a P-cell tends to be aligned with the direction of action of its downstream nucleus neuron (*5*, *51*, *52*), which implies that during a saccade in direction CS+180, the increased synchrony combines with disinhibition to entrain the nucleus neurons (*37*, *53*), producing downstream forces that are aligned with direction CS-on of the parent P-cells. As a result, the burst-pause SS rate modulation and synchronization will produce forces that oppose the direction of movement, bringing the saccade to a stop. This implies that the function of the SSs, at least in this part of the cerebellum, is not to predict sensory consequences, but to produce force.

Indeed, our results here appear consistent with this idea because we found that while the CS rates were principally modulated by visual events irrespective of whether those events were followed by movements or not. In contrast, the same visual events were undetectable in the SS rates. Rather, the SS rates were modulated only during movements.

From a computational perspective, the implication is that the P-cells may not be computing a forward model because their output is not predicting sensory consequences. Rather, the computations are more akin to a disturbance compensator, i.e., a system that learns how to alter the ongoing motor commands from a teacher (inferior olive) that provides error information in sensory coordinates (*54*).

Complex spikes and learning

We speculate that CS synchronization, coupled with rate modulation, may be the prerequisite for learning in the cerebellum. Here, we were unable to test for this because our paradigm required random primary saccades, followed by random errors, which together made it impossible to quantify the

behavioral consequences of CS synchronization on learning. However, when CSs are more synchronized, they tend to have more spikelets in their waveforms (*55*), which in turn enhances learning (*56–59*).

The CSs in this region of the cerebellum arise partly from inputs that the inferior olive receives from the superior colliculus (*60*, *61*). The collicular neurons respond following the onset of visual events, and before the onset of saccades, and indeed the P-cells show CS rate modulation in response to both events. However, the P-cells exhibit SS synchrony only during saccades, particularly those in direction CS+180. As a result, it seems likely that a movement alters the sensitivity of the olivary neurons to the sensory event that might follow it, making it to not only produce CSs in response to the secondary target, but to do so synchronously.

Methods

Data were collected from two marmosets (*Callithrix Jacchus*, male and female, 350-370 g, subjects M and R, 6 years old). The marmosets were born and raised in a colony that Prof. Xiaoqin Wang has maintained at the Johns Hopkins School of Medicine since 1996. The procedures on the marmosets were approved by the Johns Hopkins University Animal Care and Use Committee in compliance with the guidelines of the United States National Institutes of Health.

Data acquisition

Following recovery from head-post implantation surgery, the animals were trained to make saccades to visual targets and rewarded with a mixture of applesauce and lab diet (*28*). Visual targets were presented on an LCD screen (Curved MSI 32" 144 Hz - model AG32CQ) while binocular eye movements were tracked using an EyeLink-1000 eye tracking system (SR Research, USA). Timing of target presentations on the video screen was measured using a photo diode.

We performed MRI and CT imaging on each animal and used the imaging data to design an alignment system that defined trajectories from the burr hole to various locations in the cerebellar vermis (*28*), including points in lobule VI and VII. We used a piezoelectric, high precision microdrive (0.5 micron resolution) with an integrated absolute encoder (M3-LA-3.4-15 Linear smart stage, New Scale Technologies) to advance the electrode.

We recorded from the cerebellum using quartz insulated 4 fiber (tetrode) or 7 fiber (heptode) metal core (platinum/tungsten 95/05) electrodes (Thomas Recording), and 64 channel checkerboard or linear high density silicon probes (M1 and M2 probes, Cambridge Neurotech). We connected each electrode to a 32 or 64 channel head stage amplifier and digitizer (RHD2132 and RHD2164, Intan Technologies, USA), and then connected the head stage to a communication system (RHD2000 Evaluation Board, Intan Technologies, USA). Data were sampled at 30 kHz and band-pass filtered (2.5 - 7.6 kHz). We used OpenEphys (*62*) for electrophysiology data acquisition, and then used P-sort (*63*) to identify the simple and complex spikes in the heptodes and tetrodes recordings, and Kilosort and Phi (*64*) to identify the spikes for the silicon probes.

Our data set was composed of n=268 P-cells that were identified because of good isolation of CSs. Among these neurons, we also had good isolation of SSs in n=237 P-cells. We recorded from n=138 P-cells in the session in which the corrective saccade was required, and from n=130 P-cells in the session in which the corrective saccade was optional. The data for the session in which the corrective saccade was required were partially analyzed in a previous report (*29*).

Behavioral protocol

Each trial began with fixation of a center target for 200 ms, after which a primary target (0.5x0.5 deg square) appeared at one of 8 randomly selected directions at a distance of 5-6.5 deg (50 cells were recorded during sessions with 4 random directions). Onset of the primary target coincided with presentation of a distinct tone. As the animal made a saccade to this primary target, that target was erased, and a secondary target was presented at a distance of 2-2.5 deg, also at one of 8 randomly selected directions (4 directions for 50 cells). To assign a value to this erroneous outcome, in 51% of the sessions reward required both the primary and the corrective saccades, whereas in the remaining sessions reward required only the primary saccade. If reward did not require the corrective saccade, the

secondary target was presented only briefly, returning to the primary location following ~120 ms (adjusted during the recording session so that around 40% of the trials would produce a corrective saccade). Following 200 ms fixation of the final target, reward was presented with a distinct tone, and the center target was displayed.

Data analysis

All saccades, regardless of whether they were instructed by presentation of a visual target or not, were identified in the behavioral data using a velocity threshold. Saccades to primary, secondary, and central targets were labeled as targeted saccades, while all remaining saccades were labeled as task irrelevant. For the targeted saccades we computed the neurophysiological response to the presentation of the visual stimulus, as well as the response to the onset of the saccade. To compute the visual response to the secondary target, we aligned the data to the offset of the preceding primary saccade. For task irrelevant saccades, there were no visual targets and thus the response was aligned only to saccade onset.

Baseline firing rates of simple and complex spike were computed by dividing the total number of spikes by the duration of the entire recording. Instantaneous firing rates were calculated from peri-event time histograms with 1 ms bin size. We used a Savitzky–Golay filter (2nd order, 31 datapoints) to smooth the traces for visualization purposes.

CS directional tuning was computed by measuring the CS firing rates following target onset as a function of target angle with respect to the actual position of the eyes. We counted the number of CS after target onset up to saccade onset or a fixed 200 ms window, whichever happened first. Dividing the spike count by the duration of time resulted in the CS firing rate.

To compute SS population response during saccades, we began by computing the change in SS firing rate of each P-cell with respect to its baseline. Next, we labeled each saccade by measuring its direction of movement with respect to the CS-on of the P-cell. Finally, we summed the activities in all P-cells (i.e., changes with respect to baseline) for saccades in direction CS-on, CS+45, etc., using a bin size of ±25 deg.

Synchrony analysis

With multi-channel electrodes, the activity of one neuron can easily be present on multiple channels, thus giving the illusion that the two channels are picking up two distinct neurons. To guard against this, we did two things. First, after we sorted the data in each channel, we waveform triggered the data recorded by channel A by the spikes recorded on channel B. This identified the waveform of the neuron recorded by channel B on the spike recorded on channel A. We compared this cross-channel triggered waveform with the within channel triggered waveform generated by the spikes recorded by channel A. The cross-channel triggered waveform must produce a different cluster of spikes in A than the main neuron isolated by A. If there were spikes that occurred within 1 ms of each other on channels A and B, we used these coincident-spike events to trigger the waveform in A. The spikes in A that were identified to be coincident with B should look approximately the same as the non-coincident spikes in A. Examples of this approach are provided in Sedaghat-Nejad et al. (*28*).

Second, we shuffled the trials for each pair of cells, thus eliminating the simultaneity of the recording. The shuffled data produced a measure of chance level synchrony. This step was crucial

because if the spike sorting was not robust, then the spikes in one channel should contaminate the spikes in the other, resulting in a shuffled synchronization index that had a numerical value greater than one. Thus, the shuffled synchrony produced a measure of quality of the recording, as shown in Fig. 1E. We shuffled the data 50 times and computed the chance level synchronization index.

To compute synchrony, we followed the procedures described in (*29*). Briefly, we computed $\Pr(S2 = 1, S1 = 1) / [\Pr(S2 = 1) \Pr(S1 = 1)]$. This quantified whether the occurrence of a spike on channel 1 altered the probability of spikes on channel 2, corrected for probabilities expected from their average firing rates. Because channel labels 1 or 2 are interchangeable, we considered the average of the two cases as the corrected conditional probability for a pair of P-cells. Notably, the probabilities were always conditioned on visual or motor events, thus allowing the synchronization index to account for the change in the average firing rates of each cell which result from sensory or motor events. We used a 1 ms time window to compute SS synchrony, and a 20 ms time window to compute CS synchrony. Finally, we normalized the index by computing the ratio of the synchrony index as measured in the actual recording, to the synchrony index measured in the shuffled data. The shuffled data was generated by changing trial numbers for the two channels so that they were no longer simultaneous. For example, an index of 2 means that at that moment of time, it is twice as likely as chance that both neurons will fire a spike (chance level is at 1).

Statistics

To statistically analyze the population data, we computed p-values using two non-parametric methods: Wilcoxon rank sum, followed by bootstrap hypothesis testing (*65*). We report the Wilcoxon results in the manuscript, but ensured that in every case the bootstrap hypothesis testing confirmed that result. For example, to compare the CS rate response for the primary vs. secondary targets, we sampled with replacement to form a population of 50 P-cells, formed a population response, and then did this for 50 populations. We used bootstrapping to form a null distribution with zero mean from the same distribution, and then computed the probability that the mean of the measured data was different than the null hypothesis.

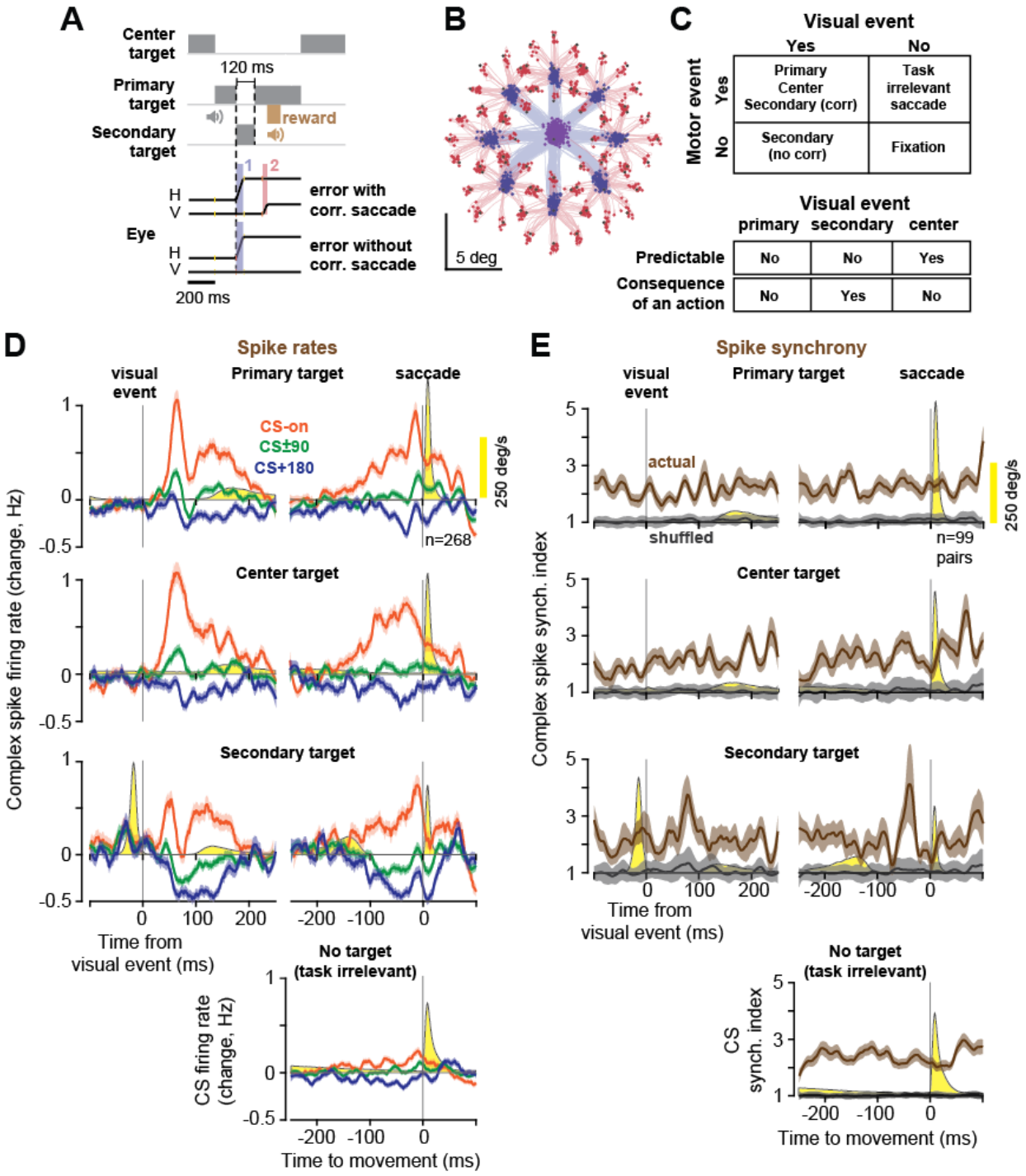

Figure 1. CS rates were modulated by various sensorimotor events, but became synchronized only in response to the erroneous consequence of a movement. **A**. Task design. **B**. Eye position traces during the primary and corrective saccades. **C**. Some but not all visual events were followed by a movement, and some but not all movements were preceded by a visual event. While both the primary and secondary targets were unpredictable, only the secondary target was the erroneous sensory consequence of a movement. **D**. Average CS firing rates as a function of direction of visual and motor events. The rates were modulated following all visual events, and before all visually guided movements. **E**. The CSs became synchronized only in response to the secondary target. Data for the secondary target are from all trials in which the subject chose to make a corrective saccade. Eye velocity is shown in yellow. Error bars are SEM.

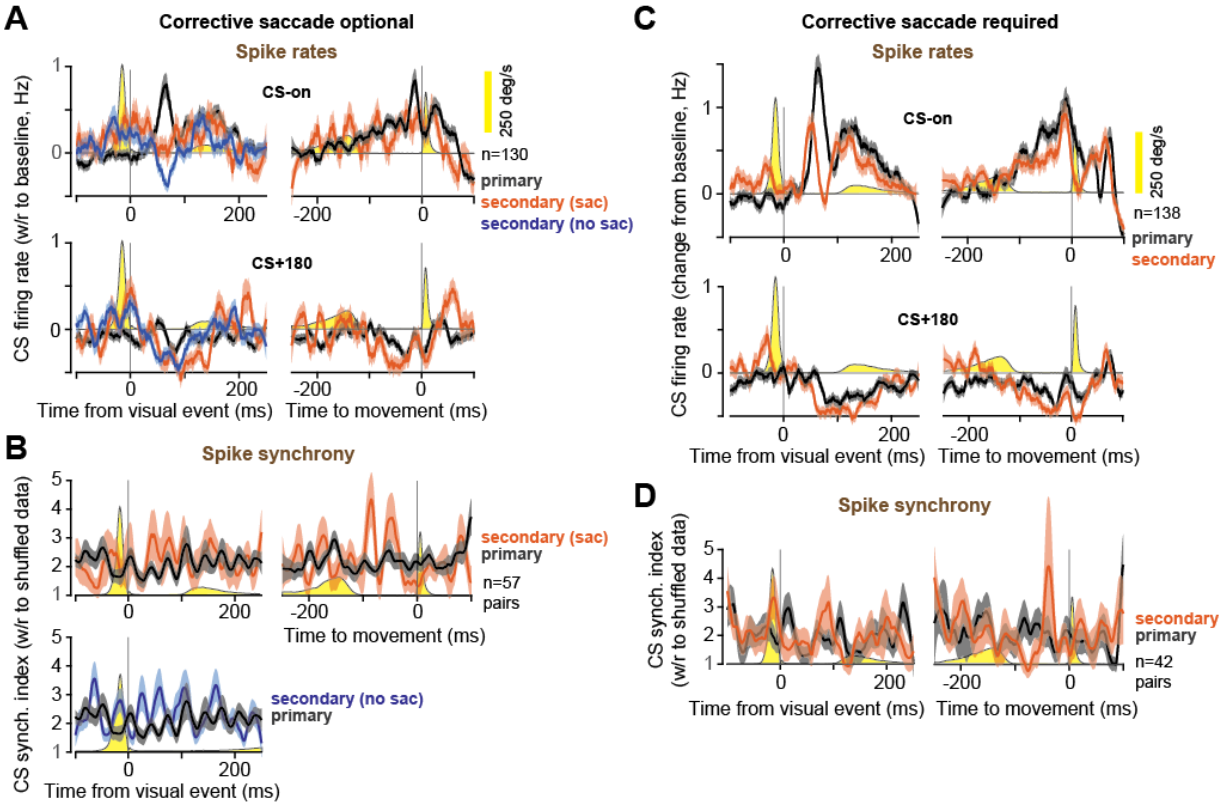

Figure 2. Devaluing the secondary target suppressed the CS rates, but the spikes became synchronized if the subject chose to make a corrective saccade. **A&B**. Data from sessions in which reward did not require making a corrective saccade. In direction CS-on, the firing rates in response to the secondary target were suppressed as compared to the primary target and suppressed further if the subject chose to ignore the stimulus. However, the CSs became synchronized if the subject chose to make a corrective saccade. Data are labeled based on whether the subject chose to ignore the secondary target (no sac) or make a corrective saccade (sac). **C&D**. Data from sessions in which the corrective saccade was required. Error bars are SEM.

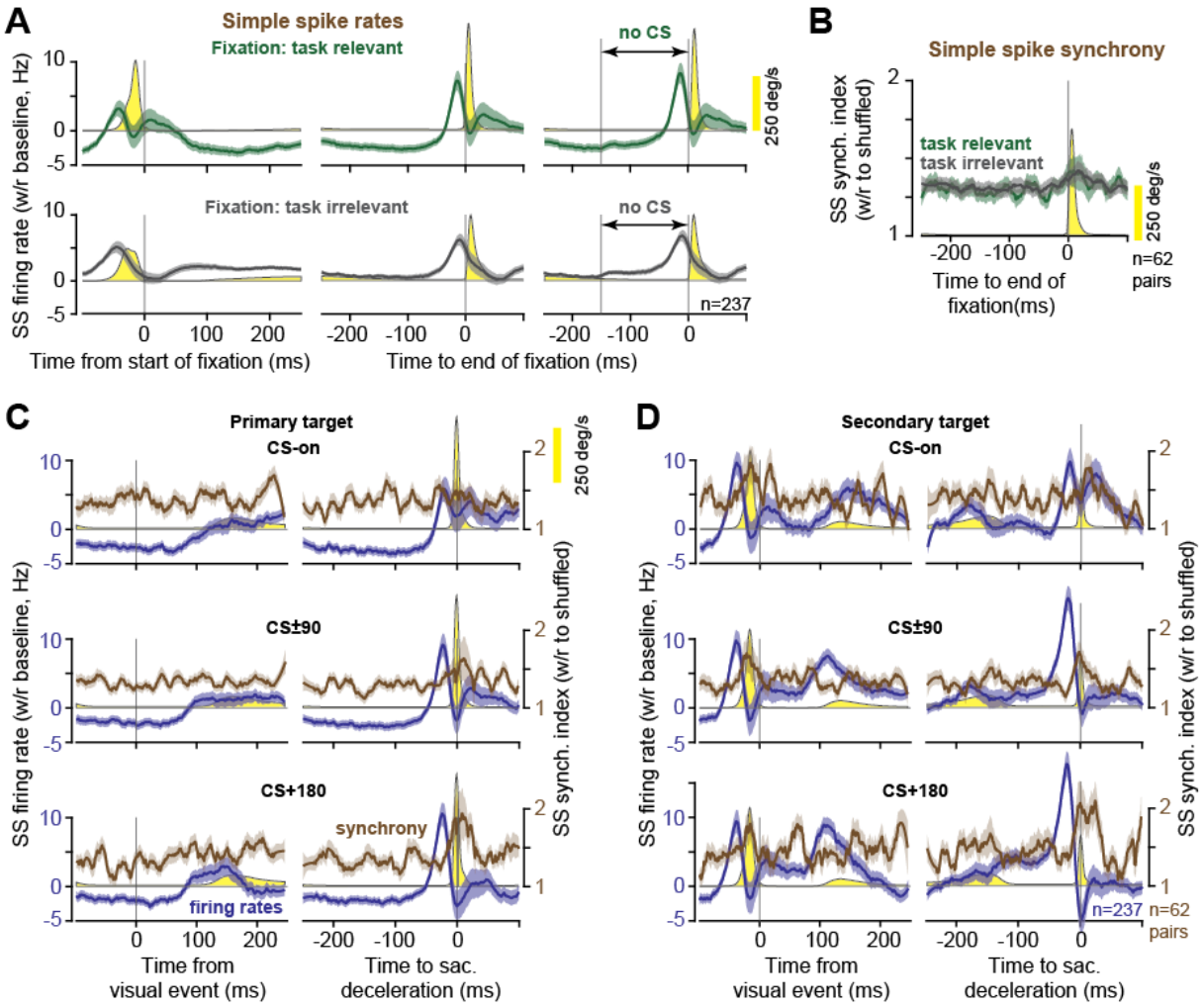

Figure 3. SSs were suppressed during fixation but modulated during movements and synchronized near movement end. **A**. SS rates were suppressed below baseline during task relevant fixations (i.e., when a visual target was present), even in trials in which no CSs were present. However, SS rates were not suppressed during task irrelevant fixation (no visual target). **B.** SS synchronization did not differ during task relevant and task irrelevant fixations. **C**. SS rates and synchrony changed in response to the primary saccade, but not in response to the primary target. **D**. SS rates and synchrony for the secondary target. Error bars are SEM.

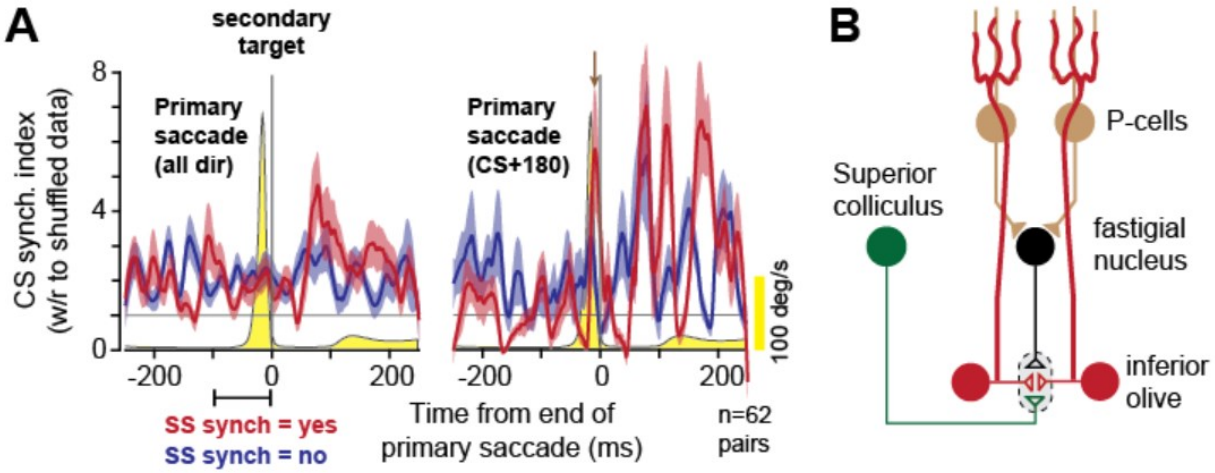

Figure 4. SS synchrony during saccades increases the likelihood of CS synchrony in response to the erroneous sensory consequences of the movement. **A**. CS synchrony index in response to the secondary target, conditioned on whether during the primary saccade that preceded it there was a synchronous SS event (100ms period before primary saccade offset). Left panel is for all primary saccades, right panel is for primary saccades in direction CS+180. Arrow notes the CS synchronous event at the end of the primary saccade. **B**. In this working model, both visual and motor related activity in the superior colliculus are reported to the inferior olive, resulting in CSs. These CSs are not synchronized. During a saccade, the P-cell SSs are modulated and synchronized, entraining the nucleus neurons, which in turn affect the state of the inferior olive. If the saccade ends with a sensory event, that event produces activity in the superior colliculus, and is reported to the inferior olive, producing a CS. However, this CS will be more likely to be synchronous with a neighboring P-cell because of the preceding input from the cerebellar nucleus to the olive. Dashed area around synapses indicates gap junctions in which subthreshold membrane oscillations in one olivary cell affects the neighboring cell.

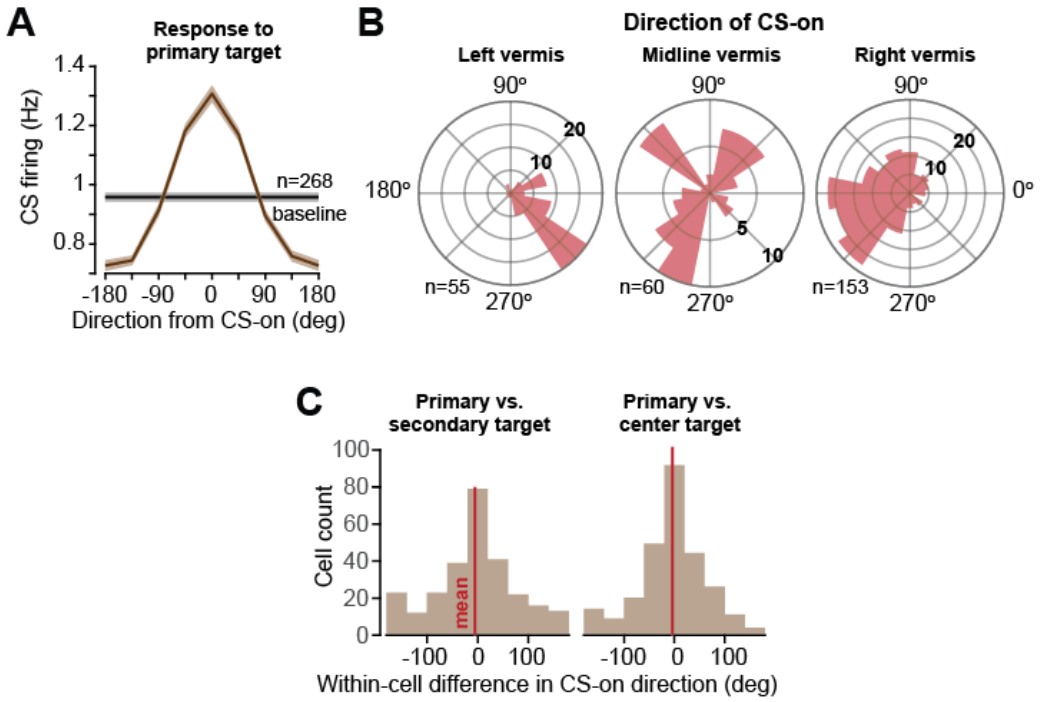

Supplementary Fig. S1. The direction of CS-on depended on the location of the P-cell in the vermis but remained consistent in response to various targets. **A**. Average CS firing rates following the presentation of the primary target, as a function of direction, aligned to direction CS-on. **B**. Distribution of CS-on as a function of location of recording in the vermis. Bin size is 15°, and the wedge at each bin represents the number of P-cells with that CS-on. **C**. Within cell difference between CS-on directions as computed following the onset of the primary target, the secondary target, and the central target. We found no systematic differences in the estimate of CS-on between various types of targets, and thus combined the response for all targets to compute the CS-on of each P-cell. Error bars are SEM.

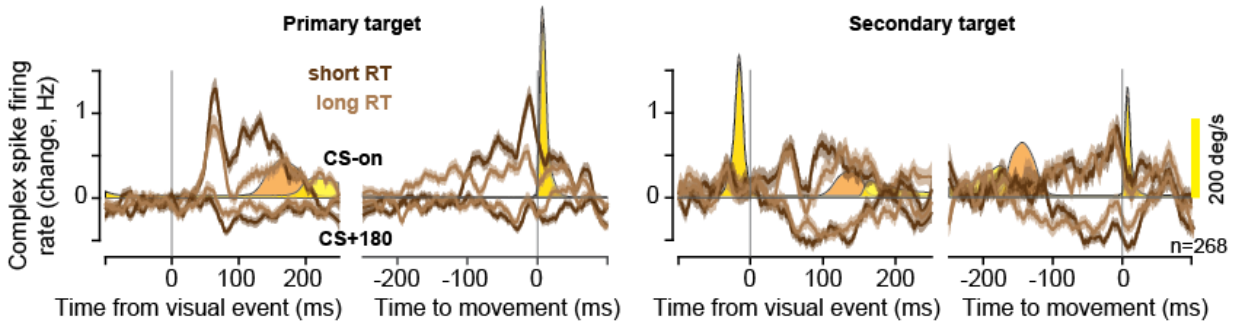

Supplementary Fig. S2. Data were separated based on the mean of the reaction time (RT) distribution for the primary (170 ms) and corrective saccades (150 ms). The CS rates were modulated following visual events, and before movements, but the strength of modulation for the primary target was weaker if the RT was longer. Darker colors indicate short RT. Error bars are SEM.

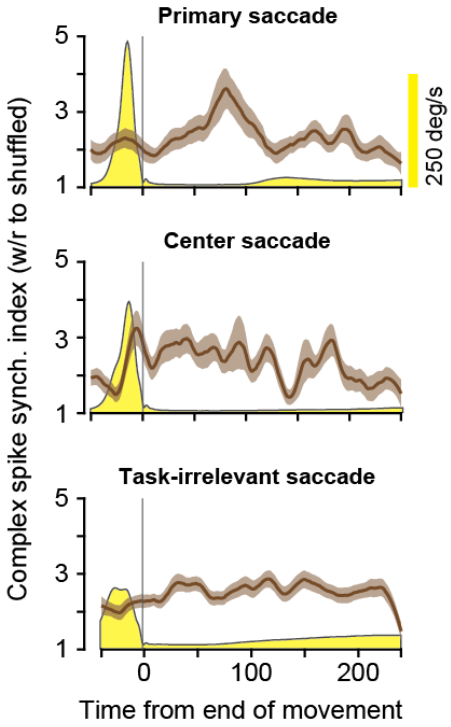

Supplementary Fig. S3. Complex spikes increased their probability of synchronization following saccades that experienced an error (primary saccade followed by the secondary target), and not other saccades (center and task irrelevant saccades). Synchronization index is computed as the ratio with respect to the shuffled data. Error bars are SEM.

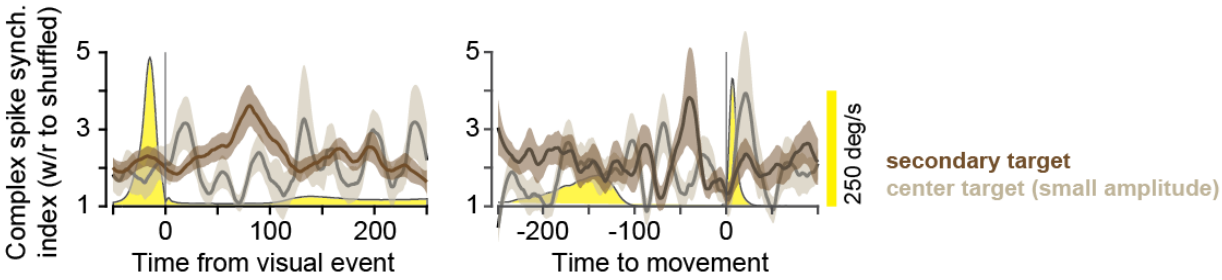

Supplementary Fig. S4. To check whether the CS synchrony for the secondary target was associated with its smaller amplitude, we sampled the center saccades that were amplitude matched with the secondary target. The probability of CS synchrony remained greater in response to the secondary target than the center target.

1. M. Ito, M. Sakurai, P. Tongroach, Climbing fibre induced depression of both mossy fibre responsiveness and glutamate sensitivity of cerebellar Purkinje cells. *J.Physiol*. **324**, 113–134 (1982).

2. J. J. Kim, D. J. Krupa, R. F. Thompson, Inhibitory cerebello-olivary projections and blocking effect in classical conditioning. *Science*. **279**, 570–573 (1998).

3. J. F. Medina, S. G. Lisberger, Links from complex spikes to local plasticity and motor learning in the cerebellum of awake-behaving monkeys. *Nat.Neurosci.* **11**, 1185–1192 (2008).

4. Y. Yang, S. G. Lisberger, Role of Plasticity at Different Sites across the Time Course of Cerebellar Motor Learning. *J. Neurosci.* **34**, 7077–7090 (2014).

5. D. J. Herzfeld, Y. Kojima, R. Soetedjo, R. Shadmehr, Encoding of error and learning to correct that error by the Purkinje cells of the cerebellum. *Nat.Neurosci.* **21**, 736–743 (2018).

6. A. S. Fanning, A. M. Shakhawat, J. L. Raymond, Population calcium responses of Purkinje cells in the oculomotor cerebellum driven by nonvisual input. *J. Neurophysiol.* **126**, 1391–1402 (2021).

7. S. Kitazawa, T. Kimura, P. B. Yin, Cerebellar complex spikes encode both destinations and errors in arm movements. *Nature*. **392**, 494 (1998).

8. R. Soetedjo, A. F. Fuchs, Complex spike activity of purkinje cells in the oculomotor vermis during behavioral adaptation of monkey saccades. *J Neurosci*. **26**, 7741–7755 (2006).

9. S. Ohmae, J. F. Medina, Climbing fibers encode a temporal-difference prediction error during cerebellar learning in mice. *Nat.Neurosci.* **18**, 1798–1803 (2015).

10. C. Ju, L. W. J. Bosman, T. M. Hoogland, A. Velauthapillai, P. Murugesan, P. Warnaar, R. M. van Genderen, M. Negrello, C. I. D. Zeeuw, Neurons of the inferior olive respond to broad classes of sensory input while subject to homeostatic control. *J. Physiol.* **597**, 2483–2514 (2019).

11. N. Larry, M. Yarkoni, A. Lixenberg, M. Joshua, Cerebellar climbing fibers encode expected reward size. *eLife*. **8** (2019), doi:10.7554/eLife.46870.

12. L. Bina, V. Romano, T. M. Hoogland, L. W. J. Bosman, C. I. De Zeeuw, Purkinje cells translate subjective salience into readiness to act and choice performance. *Cell Rep.* **37**, 110116 (2021).

13. J. P. Welsh, E. J. Lang, I. Suglhara, R. Llinas, Dynamic organization of motor control within the olivocerebellar system. *Nature*. **374**, 453–457 (1995).

14. A. L. Hewitt, L. S. Popa, T. J. Ebner, Changes in Purkinje cell simple spike encoding of reach kinematics during adaption to a mechanical perturbation. *J.Neurosci.* **35**, 1106–1124 (2015).

15. T. M. Hoogland, J. R. De Gruijl, L. Witter, C. B. Canto, C. I. De Zeeuw, Role of Synchronous Activation of Cerebellar Purkinje Cell Ensembles in Multi-joint Movement Control. *Curr. Biol.* **25**, 1157–1165 (2015).

16. W. Heffley, E. Y. Song, Z. Xu, B. N. Taylor, M. A. Hughes, A. McKinney, M. Joshua, C. Hull, Coordinated cerebellar climbing fiber activity signals learned sensorimotor predictions. *Nat. Neurosci.* **21**, 1431–1441 (2018).

17. M. J. Wagner, J. Savall, O. Hernandez, G. Mel, H. Inan, O. Rumyantsev, J. Lecoq, T. H. Kim, J. Z. Li, C. Ramakrishnan, K. Deisseroth, L. Luo, S. Ganguli, M. J. Schnitzer, A neural circuit state change underlying skilled movements. *Cell*. **184**, 3731-3747.e21 (2021).

18. R. Apps, M. Garwicz, Anatomical and physiological foundations of cerebellar information processing. *Nat.Rev.Neurosci.* **6**, 297–311 (2005).

19. F. Najafi, A. Giovannucci, S. S. Wang, J. F. Medina, Coding of stimulus strength via analog calcium signals in Purkinje cell dendrites of awake mice. *eLife*. **3**, e03663 (2014).

20. R. Soetedjo, Y. Kojima, A. F. Fuchs, Complex spike activity in the oculomotor vermis of the cerebellum: a vectorial error signal for saccade motor learning? *J.Neurophysiol.* **100**, 1949–1966 (2008).

21. T. Ishikawa, S. Tomatsu, Y. Tsunoda, J. Lee, D. S. Hoffman, S. Kakei, Releasing dentate nucleus cells from Purkinje cell inhibition generates output from the cerebrocerebellum. *PLoS.One.* **9**, e108774 (2014).

22. R. Llinás, R. A. Volkind, The olivo-cerebellar system: Functional properties as revealed by harmaline-induced tremor. *Exp. Brain Res.* **18**, 69–87 (1973).

23. V. Romano, P. Zhai, A. van der Horst, R. Mazza, T. Jacobs, S. Bauer, X. Wang, J. J. White, C. I. D. Zeeuw, Olivocerebellar control of movement symmetry. *Curr. Biol.* **32**, 654-670.e4 (2022).

24. J. L. Raymond, S. G. Lisberger, M. D. Mauk, The cerebellum: a neuronal learning machine? *Science*. **272**, 1126–1131 (1996).

25. R. Shadmehr, Population coding in the cerebellum: a machine learning perspective. *J Neurophysiol*. **124**, 2022–2051 (2020).

26. J. Wallman, A. F. Fuchs, Saccadic gain modification: visual error drives motor adaptation. *J Neurophysiol*. **80**, 2405–2416 (1998).

27. Y. W. Tseng, J. Diedrichsen, J. W. Krakauer, R. Shadmehr, A. J. Bastian, Sensory prediction errors drive cerebellum-dependent adaptation of reaching. *J.Neurophysiol.* **98**, 54–62 (2007).

28. E. Sedaghat-Nejad, D. J. Herzfeld, P. Hage, K. Karbasi, T. Palin, X. Wang, R. Shadmehr, Behavioral training of marmosets and electrophysiological recording from the cerebellum. *J.Neurophysiol.* **122**, 1502–1517 (2019).

29. E. Sedaghat-Nejad, J. S. Pi, P. Hage, M. A. Fakharian, R. Shadmehr, Synchronous spiking of cerebellar Purkinje cells during control of movements. *Proc. Natl. Acad. Sci.* **119**, e2118954119 (2022).

30. I. Sugihara, S. P. Marshall, E. J. Lang, Relationship of complex spike synchrony bands and climbing fiber projection determined by reference to aldolase C compartments in crus IIa of the rat cerebellar cortex. *JComp Neurol*. **501**, 13–29 (2007).

31. D. Kostadinov, M. Beau, M. B. Pozo, M. Hausser, Predictive and reactive reward signals conveyed by climbing fiber inputs to cerebellar Purkinje cells. *Nat.Neurosci.* **22**, 950–962 (2019).

32. T. A. Blenkinsop, E. J. Lang, Block of Inferior Olive Gap Junctional Coupling Decreases Purkinje Cell Complex Spike Synchrony and Rhythmicity. *J. Neurosci.* **26**, 1739–1748 (2006).

33. J. R. De Gruijl, T. M. Hoogland, C. I. D. Zeeuw, Behavioral Correlates of Complex Spike Synchrony in Cerebellar Microzones. *J. Neurosci.* **34**, 8937–8947 (2014).

34. Y. El-Shamayleh, Y. Kojima, R. Soetedjo, G. D. Horwitz, Selective Optogenetic Control of Purkinje Cells in Monkey Cerebellum. *Neuron*. **95**, 51-62.e4 (2017).

35. E. N. Judd, S. M. Lewis, A. L. Person, Diverse inhibitory projections from the cerebellar interposed nucleus. *eLife*. **10**, e66231 (2021).

36. Y. Lefler, Y. Yarom, M. Y. Uusisaari, Cerebellar Inhibitory Input to the Inferior Olive Decreases Electrical Coupling and Blocks Subthreshold Oscillations. *Neuron*. **81**, 1389–1400 (2014).

37. A. L. Person, I. M. Raman, Purkinje neuron synchrony elicits time-locked spiking in the cerebellar nuclei. *Nature*. **481**, 502–505 (2012).

38. E. Leznik, V. Makarenko, R. Llinás, Electrotonically Mediated Oscillatory Patterns in Neuronal Ensembles: An In Vitro Voltage-Dependent Dye-Imaging Study in the Inferior Olive. *J. Neurosci.* **22**, 2804–2815 (2002).

39. J. F. Medina, M. D. Mauk, Computer simulation of cerebellar information processing. *Nat. Neurosci*. **3**, 1205–1211 (2000).

40. J. X. Li, J. F. Medina, L. M. Frank, S. G. Lisberger, Acquisition of Neural Learning in Cerebellum and Cerebral Cortex for Smooth Pursuit Eye Movements. *J. Neurosci.* **31**, 12716–12726 (2011).

41. M. Junker, D. Endres, Z. P. Sun, P. W. Dicke, M. Giese, P. Thier, Learning from the past: A reverberation of past errors in the cerebellar climbing fiber signal. *PLOS Biol.* **16**, e2004344 (2018).

42. S. Khosrovani, R. S. V. D. Giessen, C. I. D. Zeeuw, M. T. G. De Jeu, In vivo mouse inferior olive neurons exhibit heterogeneous subthreshold oscillations and spiking patterns. *Proc. Natl. Acad. Sci.* **104**, 15911–15916 (2007).

43. L. Goffart, L. L. Chen, D. L. Sparks, Deficits in saccades and fixation during muscimol inactivation of the caudal fastigial nucleus in the rhesus monkey. *J.Neurophysiol.* **92**, 3351–3367 (2004).

44. S.-U. Lee, H.-J. Kim, J.-Y. Choi, J.-H. Choi, D. S. Zee, J.-S. Kim, Nystagmus only with fixation in the light: a rare central sign due to cerebellar malfunction. *J. Neurol.* (2022), doi:10.1007/s00415-022-11108-9.

571 45. G. Holmes, The cerebellum of man. *Brain*. **62**, 1–30 (1939).

572 46. J. X. Brooks, K. E. Cullen, The primate cerebellum selectively encodes unexpected self-motion.
573 *Curr.Biol.* **23**, 947–955 (2013).

574 47. J. Laurens, H. Meng, D. E. Angelaki, Computation of linear acceleration through an internal model
575 in the macaque cerebellum. *Nat. Neurosci.* **16**, 1701–1708 (2013).

576 48. D. J. Herzfeld, Y. Kojima, R. Soetedjo, R. Shadmehr, Encoding of action by the Purkinje cells of the
577 cerebellum. *Nature*. **526**, 439–442 (2015).

578 49. M. L. Streng, L. S. Popa, T. J. Ebner, Modulation of sensory prediction error in Purkinje cells during
579 visual feedback manipulations. *Nat. Commun.* **9**, 1099 (2018).

580 50. M. Kawato, S. Ohmae, H. Hoang, T. Sanger, 50 Years Since the Marr, Ito, and Albus Models of the
581 Cerebellum. *Neuroscience*. **462**, 151–174 (2021).

582 51. C. F. Ekerot, H. Jorntell, M. Garwicz, Functional relation between corticonuclear input and
583 movements evoked on microstimulation in cerebellar nucleus interpositus anterior in the cat.
584 *ExpBrain Res*. **106**, 365–376 (1995).

585 52. C. I. De Zeeuw, Bidirectional learning in upbound and downbound microzones of the cerebellum.
586 *Nat. Rev. Neurosci.* **22**, 92–110 (2021).

587 53. V. Gauck, D. Jaeger, The Control of Rate and Timing of Spikes in the Deep Cerebellar Nuclei by
588 Inhibition. *J. Neurosci.* **20**, 3006–3016 (2000).

589 54. M. E. Broucke, Adaptive Internal Model Theory of the Oculomotor System and the Cerebellum.
590 *IEEE Trans. Autom. Control*. **66**, 5444–5450 (2021).

591 55. E. J. Lang, T. Tang, C. Y. Suh, J. Xiao, Y. Kotsurovskyy, T. A. Blenkinsop, S. P. Marshall, I. Sugihara,
592 Modulation of Purkinje cell complex spike waveform by synchrony levels in the olivocerebellar
593 system. *Front. Syst. Neurosci.* **8** (2014) (available at
594 https://www.frontiersin.org/article/10.3389/fnsys.2014.00210).

595 56. R. S. Van Der Giessen, S. K. Koekkoek, S. van Dorp, J. R. De Gruijl, A. Cupido, S. Khosrovani, B.
596 Dortland, K. Wellershaus, J. Degen, J. Deuchars, E. C. Fuchs, H. Monyer, K. Willecke, M. T. G. De
597 Jeu, C. I. De Zeeuw, Role of Olivary Electrical Coupling in Cerebellar Motor Learning. *Neuron*. **58**,
598 599–612 (2008).

599 57. A. Mathy, S. S. Ho, J. T. Davie, I. C. Duguid, B. A. Clark, M. Hausser, Encoding of oscillations by
600 axonal bursts in inferior olive neurons. *Neuron*. **62**, 388–399 (2009).

601 58. A. Rasmussen, D. A. Jirenhed, R. Zucca, F. Johansson, P. Svensson, G. Hesslow, Number of spikes in
602 climbing fibers determines the direction of cerebellar learning. *J.Neurosci.* **33**, 13436–13440
603 (2013).

604 59. Y. Yang, S. G. Lisberger, Purkinje-cell plasticity and cerebellar motor learning are graded by
605 complex-spike duration. *Nature.* **510**, 529–532 (2014).

60. Y. Kojima, R. Soetedjo, Elimination of the error signal in the superior colliculus impairs saccade motor learning. *Proc.Natl.Acad.Sci.U.S.A*. **115**, E8987–E8995 (2018).

61. Y. Kojima, R. Soetedjo, Change in sensitivity to visual error in superior colliculus during saccade adaptation. *Sci.Rep.* **7**, 9566 (2017).

62. J. H. Siegle, A. C. Lopez, Y. A. Patel, K. Abramov, S. Ohayon, J. Voigts, Open Ephys: an open-source, plugin-based platform for multichannel electrophysiology. *JNeural Eng*. **14**, 045003 (2017).

63. E. Sedaghat-Nejad, M. A. Fakharian, J. Pi, P. Hage, Y. Kojima, R. Soetedjo, S. Ohmae, J. F. Medina, R. Shadmehr, P-sort: an open-source software for cerebellar neurophysiology. *J. Neurophysiol.* **126**, 1055–1075 (2021).

64. M. Pachitariu, N. Steinmetz, S. Kadir, M. Carandini, H. K. D, Kilosort: realtime spike-sorting for extracellular electrophysiology with hundreds of channels. *bioRxiv*, 061481 (2016).

65. V. Ventura, in *Analysis of parallel spike trains* (Springer, Boston, MA, 2010).